Effect of Dose Rate on Residual γ-H2AX Levels and Frequency of Micronuclei in X-Irradiated Mouse Lymphocytes

H. C. Turner,[1] I. Shuryak, M. Taveras, A. Bertucci, J. R. Perrier, C. Chen, C. D. Elliston, G. W. Johnson, L. B. Smilenov, S. A. Amundson and D. J. Brenner

Center for Radiological Research, Columbia University Medical Center, New York, New York 10032

Turner, H. C., Shuryak, I., Taveras, M., Bertucci, A., Perrier, J. R., Chen, C., Elliston, C. D., Johnson, G. W., Smilenov, L. B., Amundson, S. A. and Brenner, D. J. Effect of Dose Rate on Residual γ-H2AX Levels and Frequency of Micronuclei in X-Irradiated Mouse Lymphocytes. *Radiat. Res.* **183, 315–324 (2015).**

The biological risks associated with low-dose-rate (LDR) radiation exposures are not yet well defined. To assess the risk related to DNA damage, we compared the yields of two established biodosimetry end points, γ-H2AX and micronuclei (MNi), in peripheral mouse blood lymphocytes after prolonged *in vivo* exposure to LDR X rays (0.31 cGy/min) vs. acute high-dose-rate (HDR) exposure (1.03 Gy/min). C57BL/6 mice were total-body irradiated with 320 kVP X rays with doses of 0, 1.1, 2.2 and 4.45 Gy. Residual levels of total γ-H2AX fluorescence in lymphocytes isolated 24 h after the start of irradiation were assessed using indirect immunofluorescence methods. The terminal deoxynucleotidyl transferase dUTP nick end labeling (TUNEL) assay was used to determine apoptotic cell frequency in lymphocytes sampled at 24 h. Curve fitting analysis suggested that the dose response for γ-H2AX yields after acute exposures could be described by a linear dependence. In contrast, a linear-quadratic dose-response shape was more appropriate for LDR exposure (perhaps reflecting differences in repair time after different LDR doses). Dose-rate sparing effects ($P < 0.05$) were observed at doses ≤2.2 Gy, such that the acute dose γ-H2AX and TUNEL-positive cell yields were significantly larger than the equivalent LDR yields. At the 4.45 Gy dose there was no difference in γ-H2AX expression between the two dose rates, whereas there was a two- to threefold increase in apoptosis in the LDR samples compared to the equivalent 4.45 Gy acute dose. Micronuclei yields were measured at 24 h and 7 days using the *in vitro* cytokinesis-blocked micronucleus (CBMN) assay. The results showed that MNi yields increased up to 2.2 Gy with no further increase at 4.45 Gy and with no detectable dose-rate effect across the dose range 24 h or 7 days post exposure. In conclusion, the γ-H2AX biomarker showed higher sensitivity to measure dose-rate effects after low-dose LDR X rays compared to MNi formation; however, confounding factors such as variable repair times post exposure, increased cell killing and cell cycle block likely contributed to the yields of MNi with accumulating doses of ionizing radiation. © 2015 by Radiation Research Society

[1] Address for correspondence: Center for Radiological Research, Columbia University Medical Center, 630 W. 168th St. VC11-234, New York, NY 10032; e-mail: ht2231@cumc.columbia.edu.

INTRODUCTION

In the event of a large-scale radiological event, there will be a need to quickly determine, within days of radiation exposure, dose estimation and radiation risk for tens or hundreds of thousands of individuals (*1*). Many improvised nuclear device (IND) and radioactive dispersal device (RDD) scenarios involve significant portions of the dose delivered over many hours. This is self-evident for an RDD and is also true for an IND. Fallout dose is dominated in many situations by groundshine, in which radiation emission can be delivered over a significant time period – for Homeland Security planning purposes – up to 24 h (*2*). The duration of radiation exposure will vary in different situations, from fractions of a second to hours or days. According to the spectrum of dose rates used in mammalian cell radiobiology and radiotherapy described by Eric Hall (*3*), the term ''high dose rate'' is typically applied to acute exposures lasting a few minutes, and the term ''low dose rate'' is applied to protracted exposures lasting many hours or days. Generally, a given dose of sparsely ionizing radiation (e.g. X or γ rays) is less effective if it is spread over a period of hours, days or weeks as opposed to an acute dose given within a few minutes (*4, 5*). This dose-rate sparing effect has caused a great deal of speculation as to the biological risks associated with low-dose-rate (and low-dose) exposure, since many studies have been performed at higher doses and rates, with extrapolation of the risks to lower rates and doses (*6*).

Ionizing radiation is capable of inducing a wide range of damage in the DNA of an exposed cell, e.g., single- (SSB) and double-strand breaks (DSBs), DNA base alterations and DNA-DNA or DNA-protein crosslinks (*7*). It is widely accepted that DSBs are one of the most important types of DNA damage caused by ionizing radiation and other genotoxic agents, because DSBs are more difficult to repair

than many other lesions, and incorrect repair of DSBs (e.g., misrejoining of broken DNA strands from different chromosomes) can result in cytotoxic or carcinogenic genomic alterations. The dose-rate effect in mammalian cells is seen as a change in the extent of cell killing per unit dose when radiation is given at dose rates over the range of, for instance, 0.01–1 Gy/min (*8*). Early clonogenic cell survival studies in mammalian cells based on the fraction of cells surviving different rates of ionizing radiation showed that as the dose rate was lowered, cell survival increased for a given dose with the curves becoming progressively shallower and straighter (*3, 5, 9*). These findings were attributed to the repair of critical radiation damage (e.g., DSBs), which takes place during irradiation, and reduces the probability of interaction between two or more lesions that can have severe consequences, such as chromosomal aberrations (*10*). Later studies used pulsed-field gel electrophoresis (PFGE) to analyze the dose-rate effect on the induction and rejoining of DSBs (*8, 11, 12*). Although these studies indicate an apparent dose-rate effect or dose-sparing effect at lower dose rates, the results were also complicated by the lack of correlation between DSB yields and cell survival.

DSBs are induced linearly with radiation dose, with a yield of approximately 20–40 per nucleus per Gy of X or γ rays (*13*). One of the earliest steps in the radiation-induced DNA DSB repair mechanism is the rapid phosphorylation of hundreds to thousands of molecules of the histone variant H2AX by members of the phosphatidyl-inositol-3-kinase-related kinases (PIKKs) family to form a γ-H2AX focus at the site of the DSB (*14–16*). The number of radiation-induced γ-H2AX foci formed per cell nucleus has been shown to closely correspond to the number of DSBs, with each DSB yielding one focus (*17, 18*). During the past decade, the γ-H2AX assay has been applied to a variety of cell types and tissues to correlate γ-H2AX levels with DNA damage and repair (*16*). Recent studies have aimed to validate the application of the γ-H2AX protein biomarker in human population studies and for rapid triage after large-scale radiation exposure (*16, 19, 20*). Numerous γ-H2AX-based biodosimetry studies have established and validated a linear radiation dose response in human lymphocytes irradiated *ex vivo* (*20–22*) and *in vivo* (*23–25*) using immunofluorescent techniques.

DSB γ-H2AX repair kinetics show a fast and slow component after exposure to acute doses of ionizing radiation, with fast repair occurring within the first 8 h followed by slow repair over the next 24–48 h (*26, 27*). Quantification of residual levels of γ-H2AX foci *in vivo* in peripheral blood lymphocytes isolated from nonhuman primates (*28*) and more recently the minipig (*29*) exposed to acute doses of γ rays showed that residual γ-H2AX foci are proportional to the initial radiation doses. The presence of persistent or residual foci days after ionizing radiation exposure are believed to represent unrepaired DSBs or misrepaired DSBs, ongoing genomic instability, S-phase cells or apoptotic cells (*30*). Because the molecular nature of these γ-H2AX foci remains unknown, they may represent

chromosome fragments or complex DNA lesions that may be involved later on in cellular senescence and/or lead to chromosomal aberrations and micronuclei (*30–32*).

To date, few studies have examined the relationship between γ-H2AX yields and different radiation dose rates. In 2006, Kato *et al.* (*33*) investigated the number of γ-H2AX foci per cell in primary cell cultures derived from ear punch biopsies of wild-type Atm$^{+/+}$ mice after exposure to acute and protracted γ rays. Their results showed a dose-rate sparing effect, such that cells exposed to 10 cGy/h γ rays over 24 h (i.e., total dose 2.4 Gy) was similar to the residual γ-H2AX foci counts at 24 h after exposure to 1 Gy of acute γ rays. More recently, Kotenko *et al.* (*34*) measured changes in the number of radiation-induced DSBs in Chinese hamster V79 cells exposed to various dose rates of γ rays and showed that a reduction in dose rate led to a significant decrease in the number of γ-H2AX foci per cell per an absorbed dose. To our knowledge, there has not been any other study to investigate the effect of dose rate on γ-H2AX yields in peripheral blood mouse lymphocytes exposed *in vivo* to acute and protracted doses of ionizing radiation.

Another established biomarker of radiation exposure is the formation of micronuclei (MNi) in cells cultured to division (*35, 36*). The development of the cytokinesis-block (CB) technique has transformed the human-lymphocyte micronucleus assay (MN) into a reliable and precise method for assessing chromosome damage (*37*). Micronuclei are acentric chromosomal fragments or whole chromosomes lost during cell division as a result of DNA damage. Formation is dependent on DNA repair capacity and the accumulation of DNA damage. Radiation-induced chromosomal aberrations observed as MNi in peripheral blood lymphocytes are largely the result of unrepaired or misrepaired DSBs by the non-homologous end-joining pathway (*36, 38*). The dose-response relationship for micronuclei frequencies in human (*39, 40*) and mouse (*41*) peripheral blood lymphocytes (PBLs) *in vitro* after acute doses of ionizing radiation can be fitted with the linear-quadratic model. Studies aimed to investigate dose-rate effects for radiation-induced micronucleus formation in human lymphocytes reported that MNi yields decreased with decreasing dose rates (*39, 42, 43*). Bhat and Rao (*39*) showed that with decreasing dose rates the MNi response curves in CB human peripheral lymphocytes became less curvilinear, with a pure linear response of MNi induction observed at the lowest dose rate.

In the event of a mass casualty radiation incident to the human population, peripheral blood lymphocytes are more readily accessible for radiobiological measurements than other cell types. For dose assessment and rapid triage, blood sampling times are likely to vary from as early as 24 h up to a week from the start of radiation exposure. The primary goal of the current study was to compare the dose and dose-rate effect for the two established biodosimetry markers, γ-H2AX and MNi in peripheral mouse lymphocytes exposed *in vivo* to acute and protracted doses. C57BL/6 mice were exposed to total-body doses of 0–4.45 Gy of 320 kVp X

rays, delivered either at high dose rate (1.03 Gy/min) or at low dose rate (0.31 cGy/min). DNA damage repair capacity was assessed by: 1. Quantitative measurements of residual levels of total γ-H2AX fluorescence in peripheral blood lymphocytes isolated 24 h after the start of irradiation; and 2. MNi frequencies evaluated *ex vivo* using the cytokinesis-blocked micronucleus (CBMN) assay in lymphocytes isolated 24 h and 7 days post exposure.

MATERIALS AND METHODS

Animals and Irradiation

All animal husbandry and experimental procedures were conducted in accordance with applicable federal and state guidelines and approved by the Animal Care and Use Committee of Columbia University Medical Center. Male C57BL/6 mice, ages 7–9 weeks old, were obtained from Charles River Laboratories, Inc. (Wilmington, MA). Mice were housed at Columbia University animal facility with a standard 12:12 h light-dark schedule and given water and regular rodent chow ad libitum. Animals were irradiated at 8–9 weeks of age, using the X-Rad 320 X-ray machine (Precision X-Ray Inc., Branford, CT) with a fixed dose rate of 1.03 Gy/min and 0.31 cGy/min for HDR and LDR exposures, respectively. For both the HDR and LDR total-body irradiations, the mice were placed in a specially designed mouse box that consisting of 8 compartments. Each compartment was $6 \times 12.5 \times 8$ cm (w $\times$ l $\times$ h) in size and supplied with bedding, water (all-plastic water bottle) and food (gel packs).

Mice were acclimated to the mouse compartments for 24 h before irradiation. For irradiation, the box with the mice was placed in the X-ray machine and the following conditions were maintained during exposure: 1. A light-dark schedule of 12:12 h; 2. The X-ray machine temperature was kept at 22°C ($\pm$0.5°C) and humidity at 30–40% using a portable custom air conditioning system; and 3. An air exchange of 10 vol/h was maintained using a NuLine tube axial fan (cat. no. 04424883, MSC Industrial Supply Co., Melville, NY) mounted over one of the service ports of the X-ray machine. Mice were monitored through the window of the X-ray machine's door. The behavior of the animals was normal and they followed their usual cycle of sleeping, feeding and activity. For the high dose rate we used an energy of 320 kVp and current of 12.5 mA. For the low dose rate we used an energy of 320kVp and current of 0.1 mA. To achieve a dose rate of 0.31 cGy/min, a custom Thoraeus filter (1.25 mm Sn, 0.25 mm Cu, 1.5 mm Al) was used, which was placed at the maximal source-to-surface distance (SSD) of 85 cm. For a dose rate of 1.03 Gy/min, the filter was placed at 40 cm SSD.

Blood Collection and Lymphocyte Isolation

All mice were euthanized by CO_2 asphyxiation prior to blood collection. Peripheral whole blood samples were collected from each mouse by cardiac puncture; hence different mice were used for the 24 h and day 7 time points. To isolate the lymphocytes, whole blood samples (~200 μl) were diluted with 5 volumes of RPMI-1640 media (Invitrogen™, Eugene, OR). The diluted blood mix was then layered over an equal volume of lymphocyte separation media (Histopaque-1083, Invitrogen) and centrifuged at 1,300 RPM for 30 min. The lymphocyte cells formed at the interface between the separation media and plasma were resuspended in phosphate buffered saline (PBS) for the γ-H2AX and TUNEL assays or supplemented media for the CBMN assay cultures.

γ-H2AX Assay

For the immunodetection of γ-H2AX, freshly isolated lymphocytes were washed twice with PBS and fixed with ice-cold methanol for a minimum of 30 min. Slide preparations of the fixed cells were made. The cells were blocked with 3% bovine serum albumin (BSA) (Sigma-Aldrich® LLC, St. Louis, MO) for 30 min at room temperature and incubated with a rabbit polyclonal γ-H2AX (phospho S139) antibody (dilution 1:600; cat. no. ab2893, Abcam®, Cambridge, MA) for 2 h at room temperature. After three washes with PBS, the cells were visualized with a goat anti-rabbit Alexa Fluor® 488 secondary antibody (dilution 1:1,000, Invitrogen) and washed three times with PBS, and the nuclei were counterstained with DAPI [Vectashield® mounting medium with DAPI (cat. no. H-1200, Vector Laboratories, Burlingame, CA)]. Images of cells were obtained using an Olympus epifluorescence microscope (Olympus BH2-RFCA). Fluorescent images of DAPI-labeled nuclei and AF488-labeled γ-H2AX were captured separately for each dose using the Olympus epifluorescence microscope and 60× oil immersion objective. Quantification of γ-H2AX yields was determined by measuring the total γ-H2AX nuclear fluorescence per lymphocyte at a fixed exposure time of 2 s and analyzed using custom-designed image analysis software (20). Advanced apoptotic cells observed as a gross change in morphology of the DAPI-labeled nuclei were not included for analysis by the software program. The fluorescence data, generated in Microsoft Excel format as the average pixel value per nucleus, was edited for high-intensity γ-H2AX fluorescence labeling (average fluorescence >2/3 maximum fluorescence) due to fragmented nuclear DNA (44). For data acquisition, at least 200 paired lymphocyte images were captured and analyzed per data point.

Micronucleus Assay

The protocol for the micronucleus assay using isolated peripheral blood lymphocytes was adapted from Erexson and colleagues (45, 46). The isolated lymphocytes were cultured in 12-well multi-well tissue culture plates (BD Diagnostics, Franklin Lakes, NJ) containing 3 ml of RPMI-1640 media supplemented with 15% fetal bovine serum (Gibco®, Grand Island, NY), 2% Pen/Strep (Gibco) and phytohemagglutinin (PHA, cat. no. 10576-015, Gibco) at a final concentration of ~6 μg/ml to stimulate the lymphocytes to divide. The cells were cultured at 37°C in a humidified atmosphere containing 5% CO_2. After 21 h, cytochalasin B (cat. no. C6762, Sigma-Aldrich; stock solution 3,000 μg/ml dissolved in dimethysulphoxide) was added at a final concentration of 3 μg/ml to inhibit cell cytokinesis. After a total incubation period of 50 h, the mouse lymphocytes were harvested. To do this the 3 ml culture volume was transferred to a 6 ml glass centrifuge tube and the volume made up to 5 ml with PBS. The cells were spun at 1,100 rpm for 5 min after which the supernatant was removed, leaving about 0.5 ml of medium. After resuspension of the cell pellet by air bubbling using a Pasteur pipette, 4 ml of cold 0.075 *M* KCL solution (Gibco) was added and the suspension was further mixed. After 5 min, ~1 ml of ice-cold fixative mix of methanol:glacial acetic acid (3:1) was added to the cell suspension. The cells were centrifuged once more and the supernatant removed and replaced with 5 ml ice-cold fixative. At this point the cells were stored at least overnight at 4°C. Prior to slide preparation, the cells were spun and all the fixative supernatant was removed and 200 μl of freshly made fixative was added to resuspend the cells. The total cell suspension was added drop wise onto a microscope slide, allowed to air-dry and mounted using Vectashield mounting media with DAPI. Micronuclei per binucleate cell yields were examined using a fluorescent microscope (Zeiss Axioplan 2, Carl Zeiss MicroImaging Inc., Thornwood, NY) with a 40× air objective.

TUNEL Assay

Apoptosis was detected using a commercially available APO-BrdU™ TUNEL Assay Kit (cat. no. A23210, Invitrogen). The freshly isolated lymphocytes were suspended in 0.5 ml PBS (0.5 ml) and fixed with 1% (w/v) paraformaldehyde (5 ml) on ice for 15 min, centrifuged and the pelleted cells washed with PBS (5 ml). The 0.5 ml PBS cell suspension was added to ice-cold 70% (v/v) ethanol (5 ml) and stored overnight at −20°C. Briefly, to perform the TUNEL assay,
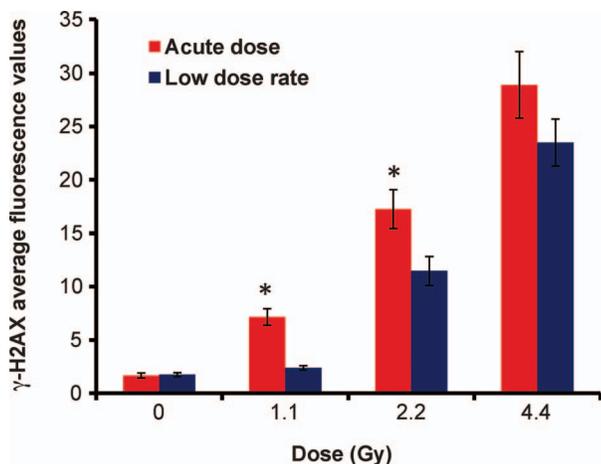
FIG. 1. Residual levels of γ-H2AX protein in mouse peripheral blood lymphocytes after acute HDR (1.03 Gy/min) and protracted LDR (0.31 cGy/min) exposure to X rays. The data presented show mean yields ± SEM measured 24 h after the start of irradiation. *Denotes statistical difference ($P \leq 0.01$).

the cells were labeled with a DNA labeling mixture containing terminal deoxynucleotidyl transferase (TdT) and the deoxythymidine analog 5-bromo-2′-deoxyuridine 5′-triphosphate (BrdUTP), conjugated with Alexa Fluor 488 dye-labeled anti-BrdU antibody. The nuclei were counterstained with propidium iodide (PI) and mounted in Vectashield® mounting medium (cat. no. H-1000, Vector Laboratories). Only nuclei fully-labeled with Alexa 488 were considered TUNEL positive within the total PI stained population using a fluorescent microscope (Carl Zeiss) and 40× air objective lens.

Preparation of Blood Smears

Blood smears were prepared with a 2 μl drop of whole blood onto a microscope slide. Once the smear was dry, the cells were fixed in ice-cold methanol for 40 min. The cells were stained with a Diff-Quik stain set (cat. no. NC9776333, Fisher Scientific, Pittsburgh, PA) used for the rapid differential staining of hematological smears to yield qualitative results similar to the Wright-Giemsa stain. After staining, the cells were mounted in rapid mounting media (Entellan®, Merck Millipore, Hatfield, PA). Each slide was issued a number, and the total number of lymphocytes present in the smear was visualized with bright field using a 40× air objective and manually counted by an experienced technologist at the Diagnostic Services, Department of Clinical Pathology and Cell Biology, Columbia University, NY. Two blood smears were prepared for each dose point from two separate mice.

Statistics

Data are presented as mean (±SEM). Data from different groups were compared by the Student's *t* test, with two-tailed $P < 0.05$ indicating statistically significant differences. To assess dose-response shape for γ-H2AX, the data were analyzed by multiple linear regression using Microsoft Excel 2010, with radiation dose and radiation dose squared as the predictors. A $P < 0.05$ for the regression coefficient for dose squared was considered sufficient evidence to suggest that the dose response is upwardly curving, rather than linear.

RESULTS

Residual Levels of γ-H2AX and Dose Response

Figure 1 shows the *in vivo* dose-rate response on residual γ-H2AX protein levels, 24 h after the start of radiation
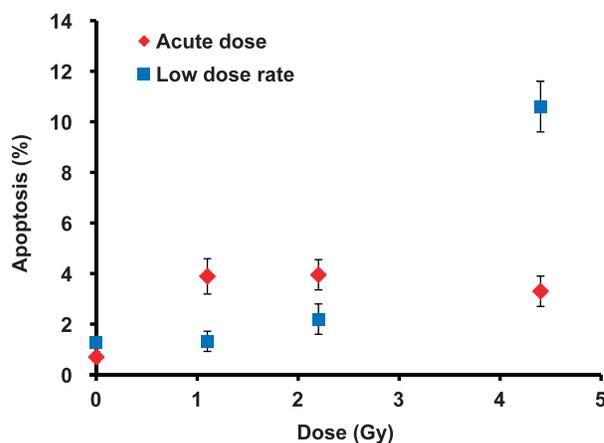
FIG. 2. Apoptosis frequency in mouse peripheral blood lymphocytes after acute HDR and protracted LDR X rays. Cells were scored for apoptosis based on TUNEL staining. The percentage of TUNEL-positive cells was determined 24 h after the start of radiation using immunofluorescence detection. Error bars are ±SEM.

exposure. The data are pooled from eight mice and the error bars show ±SEM. The mean data from at least 200 nuclei were determined for each dose point. The results show that at 1.1 and 2.2 Gy, the residual levels of γ-H2AX are significantly ($P \leq 0.01$) higher in the lymphocytes exposed to acute HDR X rays compared to the equivalent protracted LDR exposure. At 1.1 Gy LDR, the total γ-H2AX fluorescence values show close to control nonirradiated background levels. At the highest total-body dose, 4.45 Gy, there was no significant difference in the γ-H2AX yields between the two dose rates. The shapes of the dose responses for γ-H2AX yields also differed among the low and high dose rates. When the data for acute radiation doses were analyzed by multiple linear regression (see Materials and Methods section), a linear dose response was found to be adequate. This conclusion was suggested by the *P* value of 0.65 for the coefficient for dose squared. For the equivalent LDR doses, the residual levels of γ-H2AX were better described by a linear-quadratic (rather than a strictly linear) dose response: the *P* value for the regression coefficient for dose squared was 0.003.

Apoptosis Frequency

Figure 2 shows apoptosis frequency measured in mouse lymphocytes isolated 24 h after the start of irradiation. The data for each dose point was pooled from four mice (error bars show ±SEM). At least 600 cells per dose point were scored for apoptosis based on TUNEL staining. The results show a significantly larger number of apoptotic lymphocytes exposed to acute doses 1.1 Gy ($P < 0.01$) and 2.2 Gy ($P = 0.04$) compared to baseline, control levels and the equivalent LDR doses. Exposure to 4.45 Gy LDR over the 24 h period revealed two- to threefold more TUNEL-positive-labeled cells compared to acute exposure. For the acute exposures, the percentage of apoptotic cells present in each of the irradiated samples was ~4%, which was significantly ($P < 0.01$) above
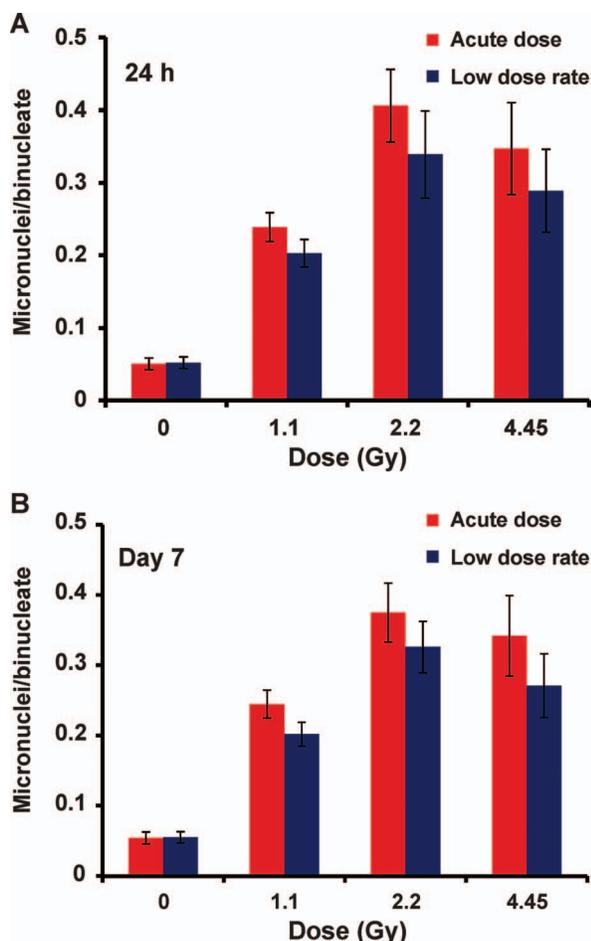
FIG. 3. Micronuclei frequency measured as the mean MNi per binucleate cell (MNi/BN) in mouse lymphocytes 24 h (panel A) and 7 days (panel B) after *in vivo* exposure to 0–4.45 Gy X rays. Error bars are ±SEM.

baseline levels. A similar trend was also observed using our semi-automated approach to eliminate oversaturated γ-H2AX-labeled apoptotic cells (see Materials and Methods section) such that similar percentages (~10%) of apoptotic cells were eliminated from all the acute HDR-irradiated samples. For the equivalent LDR exposures, the results show increasing levels of TUNEL-positive cells with increasing

dose from 1.3% (1.1 Gy), 2.3% (2.2 Gy) to 10.6% (4.45 Gy), compared with 2%, 8.4% to 26%, respectively for γ-H2AX-labeled apoptotic cells.

Micronucleus Assay Analysis

Micronuclei frequency was measured using the *in vitro* cytokinesis-blocked micronucleus assay (CBMN) and the data are presented as average number of micronuclei per binucleate cell (MNi/BN). Figure 3 shows the MNi frequency in CBMN lymphocytes for the 24 h and day 7 blood cultures (Fig. 3A and B, respectively). The data for each dose point and both time points are pooled from eight mice and the error bars show ±SEM. The results show a similar trend in the MNi dose response over the dose range 0–4.45 Gy with a monotonic increase in MNi frequency up to 2.2 Gy and no further increase at 4.45 Gy. The MNi/BN ratios were similar for the 24 h and day 7 data sets. Although the results show an apparent increased frequency for MNi formation after acute exposures, Student's two-tailed *t* test analysis showed that there was no dose-rate effect for MNi formation across the dose range examined.

Table 1 shows the distribution of the MNi formation for all the data points. As the dose increases, it is clear that the cells become increasingly less responsive to mitogen stimulation and cell division as the total number of scoreable binucleate cells decrease, particularly at the highest tested dose, 4.45 Gy. There is no dose-rate effect for binucleate cell frequency, which appears to be largely dependent on the accumulated X-ray dose. Further, these results also show that at the higher doses of 2.2 and 4.45 Gy, lymphocytes isolated on day 7 showed largely binucleate cell yields compared to the 24 h cell exposures. Qualitative observations of the DAPI-stained MNi samples indicated fewer scoreable binucleate cells and a higher proportion of necrotic and apoptotic cells in the 24 h assay samples compared to day 7. Figure 4 shows the percentage of binucleate cells containing one or more MNi, 24 h (Fig. 4A) and 7 days (Fig. 4B) after the start of irradiation. Similar to the MNi/BN dose-response curve, the data show a similar trend in MNi frequency across the dose range and no significant difference in the MNi yields between the two dose rates.

TABLE 1
Distribution of MNi in Cytokinesis-Blocked Binucleate Peripheral Blood Mouse Lymphocytes Exposed to Acute and Protracted X Rays over the Dose Range 0–4.45 Gy

		High dose rate (HDR)							Low dose rate (LDR)						
		Distribution of MNi						Total	Distribution of MNi						Total
Dose	Time	0	1	2	3	4	5	BN	0	1	2	3	4	5	BN
0 Gy	24 h	950	49	1	0	0	0	1,000	951	46	3	0	0	0	1,000
	Day 7	949	48	3	0	0	0	1,000	966	52	2	0	0	0	1,020
1 Gy	24 h	502	110	16	3	0	0	631	441	91	8	1	0	0	541
	Day 7	537	121	16	3	1	0	678	574	111	12	2	0	0	699
2 Gy	24 h	122	46	9	3	0	0	180	145	37	8	3	1	0	194
	Day 7	207	63	14	3	1	1	289	224	62	12	3	1	0	302
4 Gy	24 h	62	21	3	1	0	0	87	88	19	6	1	0	0	114
	Day 7	80	24	7	0	0	0	111	102	26	5	0	0	0	133
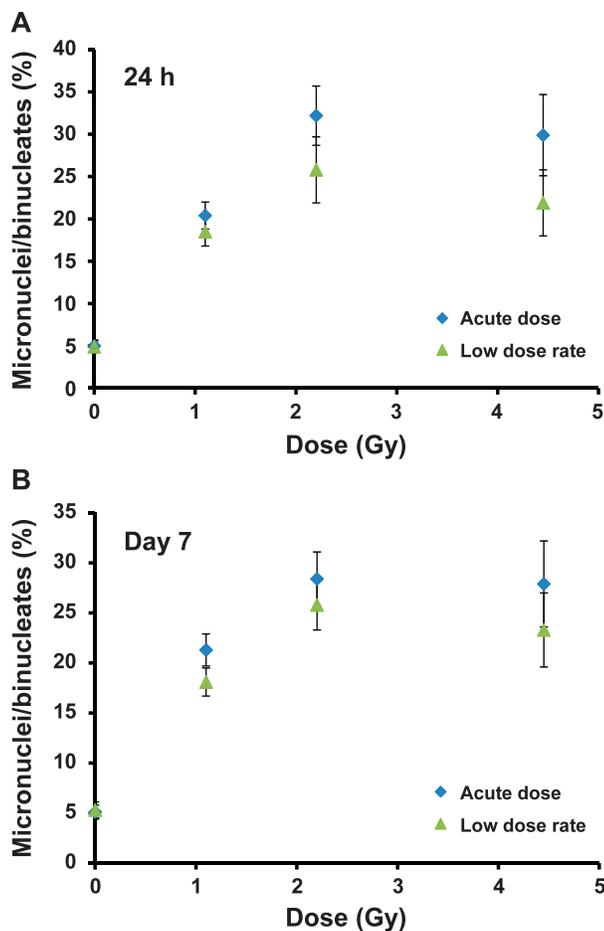
FIG. 4. Total percentage of micronucleated binucleate cells after acute HDR and protracted LDR exposure to X rays, 24 h (panel A) and 7 days (panel B) after *in vivo* exposure to 0–4.45 Gy X rays. Error bars are ±SEM.

Blood Counts

The mean (error bars show ±SEM, n = 2 mice for each dose point) total blood lymphocyte counts were analyzed from at least two blood smears per dose point. The results revealed approximately 773 ± 104 mononuclear lymphocytes at 0 Gy compared to 60 ± 18 (1.1 Gy), 42 ± 10 (2.2 Gy) and 34 ± 8 (4.45 Gy) after HDR X-ray exposures and 43 ± 23 (1.1 Gy), 63 ± 11 (2.2 Gy) and 44 ± 5 (4.45 Gy) lymphocytes after LDR exposures. For acute exposures, blood smear analysis showed a small dose-dependent decrease in lymphocyte numbers, although LDR exposures do not show a defined dose-dependent change. However, there is a dramatic decrease in peripheral blood lymphocytes from all the irradiated mice compared to the control, nonirradiated blood samples.

DISCUSSION

In the current study, we compared the effect of acute and protracted X-ray exposures on γ-H2AX yields in peripheral blood mouse lymphocytes *in vivo* measured 24 h after the start of irradiation. The extent of DNA DSB damage and repair was quantified by the determination of residual γ-H2AX levels measured as the total γ-H2AX fluorescence per cell nuclei. All acute exposures received ~24 h of repair time post exposure, while the repair times for the low-dose LDR exposures were varied and dependent on the total dose. The results show that for both dose rates, residual γ-H2AX yields increased in a dose-dependent manner over the dose range 0–4.45 Gy (Fig. 1). The response after acute exposures was linear, whereas for the LDR exposures there was a quadratic component. The quadratic component in the LDR dose response may be due to differences in time available for repair (between the time when irradiation ended and when the damage assay was performed): for lower cumulative LDR doses, the time available for repair was longer, than for higher LDR doses. This repair time effect may explain the apparently counterintuitive finding that the LDR dose response is curved, whereas the HDR dose response is not, instead of the other way around (as would be suggested by classical linear-quadratic theory). At 1.1 and 2.2 Gy doses, the residual levels of total γ-H2AX fluorescence were significantly ($P \leq 0.01$) greater after acute X-ray exposure compared to LDR exposure, highlighting a dose-rate sparing effect after protracted exposure. The residual γ-H2AX levels in the 1.1 Gy LDR samples were the closest to control, nonirradiated baseline levels and thus, contributed to the LDR curve's deviation from linearity. Although it is not possible to directly compare the DSB repair rates for each data point due to the variable repair times post exposure, the fact that the 1.1 and 2.2 Gy LDR samples received less time to repair compared to the equivalent acute dose exposures suggests a faster and/or more efficient activation of DNA DSB repair during protracted exposures. The reduced γ-H2AX yields may be due to a reduced probability for the interaction of the DSB lesions giving way to more efficient DSB repair at lower doses and dose rates, compared to exposure with an equivalent dose of high-density, high-dose-rate X rays. At 4.45 Gy there was no significant difference in the γ-H2AX yields between the two dose rates. This may be due largely to the fact that the cells exposed to 4.45 Gy LDR X rays received no repair time after the end of radiation treatment compared to the equivalent acute dose. This would certainly be true for the induction of DSBs formed towards the end of the irradiation time. However, the exponential high levels of residual γ-H2AX in the 4.45 Gy LDR samples clearly show that the rate of induction of DSBs in a large proportion of the exposed lymphocytes significantly exceeded their repair over the 24 h exposure time. Despite the lack of linearity for the γ-H2AX LDR exposures, the current results suggest that γ-H2AX is a sensitive assay for measuring low-dose and LDR effects 24 h after exposure.

Apoptosis is a defense mechanism to eliminate cells with unrepaired DNA damage. DNA fragmentation is a hallmark of radiation-induced apoptosis. Human lymphocytes have been shown to undergo apoptosis in a time-, dose- and dose-rate-dependent manner (*42, 47*). Further, γ-H2AX has been

shown to appear during apoptosis concurrently with the initial appearance of high molecular weight DNA fragments (*44*). Therefore, residual levels of apoptosis in the irradiated samples at 24 h are a potential confounding factor for the γ-H2AX total fluorescence analysis. To assess the extent of apoptosis in the irradiated samples, we compared the percentage of γ-H2AX-labeled apoptotic cells with the percentage of TUNEL-positive cells for each data point. The TUNEL assay is used to detect apoptotic cells that undergo extensive DNA degradation during the late stages of apoptosis (*48*) whereas our semiquantitative approach to remove intensely γ-H2AX-labeled apoptotic cells is likely to include cells in the early to late stages of apoptosis; hence the increased number of lymphocyte cells eliminated from the γ-H2AX analysis.

For the acute HDR exposures, the results showed that the percentage of apoptotic cells present in the irradiated samples was similar for each dose, whereas for LDR exposures, the results showed an increasing number of apoptotic cells with increasing dose. TUNEL assay data (Fig. 2) showed a significant dose-sparing effect after 1.1 Gy ($P < 0.01$) and 2.2 Gy ($P = 0.04$) LDR X rays, whereas at 4.45 Gy, a dramatic induction of apoptosis was measured in the LDR samples that was two- and threefold higher than the equivalent acute dose. Although the presence of fewer cells with apoptotic characteristics in the 1.1 and 2.2 Gy LDR exposed samples coincided with reduced γ-H2AX yields, the dose response for TUNEL-positive cells was not linear, suggesting that it is unlikely that the levels of residual apoptosis are directly due to the induction of DSBs. For the 4.45 Gy acute samples, we speculate that the acute dose X rays are likely to induce peak apoptosis earlier during the 24 h repair time, leading to increased cell death and clearing of the highly damaged cells from the peripheral blood circulation prior to collection. Whereas for the 4.45 Gy LDR samples, the peak time for the induction of apoptosis was closer to 24 h, hence the significantly higher levels of apoptosis measured at this time. Previous studies in mouse lymphocytes exposed *in vitro* after a 2 Gy acute dose of γ rays have shown that radiation-induced apoptosis peaked at 8 h (*49*). More recently, Bogdandi *et al.* (*50*) reported that apoptosis was highest at 4 h and declined by 24 h in isolated mouse splenocytes after *in vivo* total-body irradiation up to 2 Gy γ rays.

MNi frequency was determined in peripheral lympho-cytes isolated 24 h and 7 days after the start of *in vivo* irradiation using the *in vitro* CBMN assay. We used the mitogen PHA to selectively stimulate isolated mature T cells to divide. The results showed that MNi yields per binucleate cell for both dose rates and time points increased monotonically up to 2.2 Gy with no further increase in MNi formation at 4.45 Gy (Fig. 3). Two-tailed *t* test analysis showed that there was no significant dose-rate effect for MNi frequency across the dose range examined. Since the error bars in general overlap between 2.2 and 4.45 Gy doses, this would suggest that the effect is saturating at 2.2

Gy and no further effect is being observed at the higher dose. This may be due to a higher percentage of the cells becoming senescent, going through apoptosis or necrosis as the dose increases and leading to a smaller number of binucleate cells being analyzed. Interestingly, there is an apparent increase in the number of scoreable cells in the day 7 cultures compared to 24 h. As noted in the Results section, an increase in the presence of necrotic and apoptotic cells was observed in the 24 h cultures, indicating that a larger proportion of the cells have initiated radiation-induced cell death during the assay culture time. Notwithstanding, the dose response for MNi frequency was similar between the time points.

Plotting the data to show the percentage of micro-nucleated binucleates in each sample (Fig. 4) showed that the general trend as noted in Fig. 4 is that acute exposures induce a higher level of MNi compared to LDR exposures, although the results did not show a statistically significant difference. As with the MNi/BN measurements, there is very little difference in the dose-response curve obtained for MNi formation at 24 h or 7 days post exposure, thereby widening the appeal for the use of this biomarker to determine individual dose estimates up to a week after *in vivo* ionizing radiation exposure. An explanation for this finding, according to Fenech and colleagues, is that the migration of damaged bone marrow and thymus-derived progenitor lymphocytes into the blood stream will likely contribute to the MNi yields measured on day 7 (*51*). To the best of our knowledge, no dose rate studies have been performed in peripheral blood mouse lymphocytes exposed to ionizing radiation. However, previous studies in human lymphocytes exposed *ex vivo* to different dose rates of γ ray (*39*) and X ray (*43*) have shown a significant dose-rate effect in the high-dose regions, where the MNi yields decreased with decreasing dose rates, while the response remained almost the same as that of acute exposure at the low-dose region, i.e., up to 1 Gy (*39*). The dose-rate effect was attributed to the rate at which sublethal damage is repaired.

In the current study, we speculate that the absence of a dose-rate effect for MNi frequency at either time point is likely due to a combination effect of different repair times post exposure, increased cell killing and cell cycle arrest. These confounding factors are more apparent at the highest dose. At the lower total-body doses, we might also consider that the CBMN assay is not as sensitive as the γ-H2AX biomarker to detect dose-rate effects. These findings might also suggest (albeit lacking any direct evidence) that the repair kinetics for the subset of DSBs that result in MNi may be insensitive to dose rate. To date, few studies have measured a dose-response relationship for MNi formation in cytochalasin-blocked mouse lymphocytes after treatment with acute dose X rays (*41, 51*) and γ rays (*52, 53*). This is largely due to the challenge of stimulating peripheral mouse lymphocytes to divide with adequate and consistent mitotic activity for cytogenetic studies (*45, 54*). Although Erexson

and colleagues (*52*) reported in one of their studies a dose-dependent increase in MNi in binucleated mouse lymphocytes up to 4 Gy with ^{60}Co gamma radiation, other studies have largely obtained a dose response for MNi yields up to 2 Gy (*51*) and 3 Gy (*41, 53*).

A snapshot of the circulating blood lymphocytes from blood smear preparations indicated that overall there was a dramatic reduction in lymphocyte cells for each dose point (LDR and HDR) compared to the control, nonirradiated mice, suggesting that mouse T-cell lymphocytes are radiosensitive to low doses and dose rates of X rays. Previous studies have shown that mouse T-cell lymphocytes are radiosensitive to low doses of X rays (*55*) and that the decrease in T-cell counts postirradiation is dose-rate independent (*56, 57*). Our results showed a small dose-dependent loss in counts for the acute exposures and no defined dose-dependent change for the LDR exposures. We now propose that more extensive studies are required to further investigate this response pattern. Although the reduction in the number of circulating peripheral blood lymphocytes across the dose range did not prove to be a limiting factor for the γ-H2AX or the TUNEL assay analyses, this may not be the case for the CBMN assay and blood lymphocytes exposed with the high-dose X rays. For future studies, we will consider the use of larger volumes of blood for the mouse CBMN assay as well as the use of other animal models for comparison.

CONCLUSIONS

To our knowledge this is the first study to directly compare the effect of dose and dose-rate effects of two biodosimetry markers, γ-H2AX and MNi, from the same peripheral mouse lymphocyte cell samples exposed to *in vivo* ionizing radiation. In this work, we have described several potential confounding factors that may contribute to the measurement of γ-H2AX and MNi yields and lack thereof dose-rate effects after exposure to acute and protracted X rays. Despite several complicating factors, the study results suggest the following generalizations: 1. Reduced yields of total γ-H2AX fluorescent protein and the percentage of apoptotic cells after LDR vs. HDR exposure at X-ray doses ≤2.2 Gy may suggest more efficient and enhanced repair kinetics for radiation-induced DSBs; 2. The dose-rate sparing effect at doses ≤2.2 Gy may explain the difference in γ-H2AX dose-response shape for HDR vs. LDR exposures: the LDR dose-response curve appears to have a quadratic component because the γ-H2AX level at 1.1 Gy was very close to the nonirradiated baseline level; 3. The combined effect of different repair times post exposure, increased cell killing and cell cycle arrest may contribute to the lack of dose effects for MNi frequency; and 4. Total-body dose estimates based on the assessment of MNi yields may be reliable up to one week post exposure. To this end, we consider that the combined use of these two established biomarkers may offer the best approach to improve dose estimates for rapid triage in individuals exposed to different doses and dose rates of ionizing radiation.

REFERENCES

1. Grace MB, Moyer BR, Prasher J, Cliffer KD, Ramakrishnan N, Kaminski J, et al. Rapid radiation dose assessment for radiological public health emergencies: roles of NIAID and BARDA. Health Phys 2010; 98:172–8.

2. National planning scenarios, version 21.3. Washington DC: Homeland Security Council; 2006. (http://bit.ly/1udh6Y5)

3. Hall EJ. Radiation dose-rate: a factor of importance in radiobiology and radiotherapy. Br J Radiol 1972; 45:81–97.

4. Hall EJ, Brenner DJ. The dose-rate effect revisited: radiobiological considerations of importance in radiotherapy. Int J Radiat Oncol Biol Phys 1991; 21:1403–14.

5. Hall EJ, Bedford JS. Dose rate: its effect on the survival of HeLa cells irradiated with gamma rays. Radiat Res 1964; 22:305–15.

6. Sorensen KJ, Zetterberg LA, Nelson DO, Grawe J, Tucker JD. The in vivo dose rate effect of chronic gamma radiation in mice: translocation and micronucleus analyses. Mutat Res 2000; 457:125–36.

7. Smith LE, Nagar S, Kim GJ, Morgan WF. Radiation-induced genomic instability: radiation quality and dose response. Health Phys 2003; 85:23–9.

8. Ruiz de Almodovar JM, Bush C, Peacock JH, Steel GG, Whitaker SJ, McMillan TJ. Dose-rate effect for DNA damage induced by ionizing radiation in human tumor cells. Radiat Res 1994; 138:S93–6.

9. Ben-Hur E, Elkind MM. Thermally enhanced radioresponse of cultured Chinese hamster cells: damage and repair of single-stranded DNA and a DNA complex. Radiat Res 1974; 59:484–95.

10. Frankenberg-Schwager M, Frankenberg D, Blocher D, Adamczyk C. Effect of dose rate on the induction of DNA double-strand breaks in eucaryotic cells. Radiat Res 1981; 87:710–7.

11. Boucher D, Hindo J, Averbeck D. Increased repair of gamma-induced DNA double-strand breaks at lower dose-rate in CHO cells. Can J Physiol Pharmacol 2004; 82:125–32.

12. Dhermain F, Dardalhon M, Queinnec E, Averbeck D. Induction of double-strand breaks in Chinese hamster ovary cells at two different dose rates of gamma-irradiation. Mutat Res 1995; 336:161–7.

13. Goodhead DT. Initial events in the cellular effects of ionizing radiations: clustered damage in DNA. Int J Radiat Biol 1994; 65:7–17.

14. Bonner WM, Redon CE, Dickey JS, Nakamura AJ, Sedelnikova OA, Solier S, et al. GammaH2AX and cancer. Nat Rev Cancer 2008; 8:957–67.

15. Rogakou EP, Pilch DR, Orr AH, Ivanova VS, Bonner WM. DNA double-stranded breaks induce histone H2AX phosphorylation on serine 139. J Biol Chem 1998; 273:5858–68.

16. Valdiglesias V, Giunta S, Fenech M, Neri M, Bonassi S. gammaH2AX as a marker of DNA double strand breaks and

genomic instability in human population studies. Mutat Res 2013; 753:24–40.

17. Rogakou EP, Boon C, Redon C, Bonner WM. Megabase chromatin domains involved in DNA double-strand breaks in vivo. J Cell Biol 1999; 146:905–16.

18. Sedelnikova OA, Rogakou EP, Panyutin IG, Bonner WM. Quantitative detection of (125)IdU-induced DNA double-strand breaks with gamma-H2AX antibody. Radiat Res 2002; 158:486–92.

19. Rothkamm K, Horn S, Scherthan H, Rossler U, De Amicis A, Barnard S, et al. Laboratory intercomparison on the gamma-H2AX foci assay. Radiat Res 2013; 180:149–55.

20. Turner HC, Brenner DJ, Chen Y, Bertucci A, Zhang J, Wang H, et al. Adapting the gamma-H2AX assay for automated processing in human lymphocytes. 1. Technological aspects. Radiat Res 2011; 175:282–90.

21. Andrievski A, Wilkins RC. The response of gamma-H2AX in human lymphocytes and lymphocytes subsets measured in whole blood cultures. Int J Radiat Biol 2009; 85:369–76.

22. Rothkamm K, Lobrich M. Evidence for a lack of DNA double-strand break repair in human cells exposed to very low x-ray doses. Proc Natl Acad Sci U S A 2003; 100:5057–62.

23. Halm BM, Franke AA, Lai JF, Turner HC, Brenner DJ, Zohrabian VM, et al. gamma-H2AX foci are increased in lymphocytes in vivo in young children 1 h after very low-dose X-irradiation: a pilot study. Pediatr Radiol 2014; 44:1310–7.

24. Lobrich M, Rief N, Kuhne M, Heckmann M, Fleckenstein J, Rube C, et al. In vivo formation and repair of DNA double-strand breaks after computed tomography examinations. Proc Natl Acad Sci U S A 2005; 102:8984–9.

25. Sak A, Grehl S, Erichsen P, Engelhard M, Grannass A, Levegrun S, et al. gamma-H2AX foci formation in peripheral blood lymphocytes of tumor patients after local radiotherapy to different sites of the body: dependence on the dose-distribution, irradiated site and time from start of treatment. Int J Radiat Biol 2007; 83:639–52.

26. Rothkamm K, Horn S. gamma-H2AX as protein biomarker for radiation exposure. Ann Ist Super Sanita 2009; 45:265–71.

27. Turner HC, Sharma P, Perrier JR, Bertucci A, Smilenov L, Johnson G, et al. The RABiT: high-throughput technology for assessing global DSB repair. Radiat Environ Biophys 2014; 53:265–72.

28. Redon CE, Nakamura AJ, Gouliaeva K, Rahman A, Blakely WF, Bonner WM. The use of gamma-H2AX as a biodosimeter for total-body radiation exposure in non-human primates. PloS One 2010; 5:e15544.

29. Moroni M, Maeda D, Whitnall MH, Bonner WM, Redon CE. Evaluation of the gamma-H2AX assay for radiation biodosimetry in a swine model. Int J Mol Sci 2013; 14:14119–35.

30. Bhogal N, Kaspler P, Jalali F, Hyrien O, Chen R, Hill RP, et al. Late residual gamma-H2AX foci in murine skin are dose responsive and predict radiosensitivity in vivo. Radiat Res 2010; 173:1–9.

31. Paull TT, Rogakou EP, Yamazaki V, Kirchgessner CU, Gellert M, Bonner WM. A critical role for histone H2AX in recruitment of repair factors to nuclear foci after DNA damage. Curr Biol 2000; 10:886–95.

32. Suzuki M, Suzuki K, Kodama S, Watanabe M. Phosphorylated histone H2AX foci persist on rejoined mitotic chromosomes in normal human diploid cells exposed to ionizing radiation. Radiat Res 2006; 165:269–76.

33. Kato TA, Nagasawa H, Weil MM, Genik PC, Little JB, Bedford JS. gamma-H2AX foci after low-dose-rate irradiation reveal atm haploinsufficiency in mice. Radiat Res 2006; 166:47–54.

34. Kotenko KV, Bushmanov AY, Ozerov IV, Guryev DV, Anchishkina NA, Smetanina NM, et al. Changes in the number of double-strand DNA breaks in Chinese hamster V79 cells exposed to gamma-radiation with different dose rates. Int J Mol Sci 2013; 14:13719–26.

35. Fenech M, Morley AA. Measurement of micronuclei in lymphocytes. Mutat Res 1985; 147:29–36.

36. Vral A, Fenech M, Thierens H. The micronucleus assay as a biological dosimeter of in vivo ionising radiation exposure. Mutagenesis 2011; 26:11–7.

37. Fenech M. The cytokinesis-block micronucleus technique: a detailed description of the method and its application to genotoxicity studies in human populations. Mutat Res 1993; 285:35–44.

38. Iliakis G, Wang H, Perrault AR, Boecker W, Rosidi B, Windhofer F, et al. Mechanisms of DNA double strand break repair and chromosome aberration formation. Cytogenet Genome Res 2004; 104:14–20.

39. Bhat NN, Rao BS. Dose rate effect on micronuclei induction in cytokinesis blocked human peripheral blood lymphocytes. Radiat Prot Dosimetry 2003; 106:45–52.

40. Willems P, August L, Slabbert J, Romm H, Oestreicher U, Thierens H, et al. Automated micronucleus (MN) scoring for population triage in case of large scale radiation events. Int J Radiat Biol 2010; 86:2–11.

41. Erexson GL, Kligerman AD, Bryant MF, Sontag MR, Halperin EC. Induction of micronuclei by X-radiation in human, mouse and rat peripheral blood lymphocytes. Mutat Res 1991; 253:193–8.

42. Boreham DR, Dolling JA, Maves SR, Siwarungsun N, Mitchel RE. Dose-rate effects for apoptosis and micronucleus formation in gamma-irradiated human lymphocytes. Radiat Res 2000; 153:579–86.

43. Vral A, Thierens H, De Ridder L. Study of dose-rate and split-dose effects on the in vitro micronucleus yield in human lymphocytes exposed to X-rays. Int J Radiat Biol 1992; 61:777–84.

44. Rogakou EP, Nieves-Neira W, Boon C, Pommier Y, Bonner WM. Initiation of DNA fragmentation during apoptosis induces phosphorylation of H2AX histone at serine 139. J Biol Chem 2000; 275:9390–5.

45. Erexson GL, Kligerman AD. A modified mouse peripheral blood lymphocyte culture system for cytogenetic analysis. Environ Mol Mutagen 1987; 10:377–86.

46. Erexson GL, Kligerman AD, Allen JW. Diaziquone-induced micronuclei in cytochalasin B-blocked mouse peripheral blood lymphocytes. Mutat Res 1987; 178:117–22.

47. Payne CM, Bjore CG, Jr., Schultz DA. Change in the frequency of apoptosis after low- and high-dose X-irradiation of human lymphocytes. J Leukoc Biol 1992; 52:433–40.

48. Kyrylkova K, Kyryachenko S, Leid M, Kioussi C. Detection of apoptosis by TUNEL assay. Methods Mol Biol 2012; 887:41–7.

49. Lemon JA, Rollo CD, McFarlane NM, Boreham DR. Radiation-induced apoptosis in mouse lymphocytes is modified by a complex dietary supplement: the effect of genotype and gender. Mutagenesis 2008; 23:465–72.

50. Bogdandi EN, Balogh A, Felgyinszki N, Szatmari T, Persa E, Hildebrandt G, et al. Effects of low-dose radiation on the immune system of mice after total-body irradiation. Radiat Res 2010; 174:480–9.

51. Fenech MF, Dunaiski V, Osborne Y, Morley AA. The cytokinesis-block micronucleus assay as a biological dosimeter in spleen and peripheral blood lymphocytes of the mouse following acute whole-body irradiation. Mutat Res 1991; 263:119–26.

52. Erexson GL, Kligerman AD, Halperin EC, Honore GM, Allen JW. Micronuclei in binucleated lymphocytes of mice following exposure to gamma radiation. Environ Mol Mutagen 1989; 13:128–32.

53. Chen Y, Tsai Y, Nowak I, Wang N, Hyrien O, Wilkins R, et al.

Validating high-throughput micronucleus analysis of peripheral reticulocytes for radiation biodosimetry: benchmark against dicentric and CBMN assays in a mouse model. Health Phys 2010; 98:218–27.

54. Kim SH, Han DU, Lim JT, Jo SK, Kim TH. Induction of micronuclei in human, goat, rabbit peripheral blood lymphocytes and mouse splenic lymphocytes irradiated in vitro with gamma radiation. Mutat Res 1997; 393:207–14.

55. Anderson RE, Williams WL. Radiosensitivity of T and B lymphocytes. V. Effects of whole-body irradiation on numbers of recirculating T cells and sensitization to primary skin grafts in mice. Am J Pathol 1977; 89:367–78.

56. Fujikawa K, Hasegawa Y, Matsuzawa S, Fukunaga A, Itoh T, Kondo S. Dose and dose-rate effects of X rays and fission neutrons on lymphocyte apoptosis in p53(+/+) and p53(–/–) mice. J Radiat Res 2000; 41:113–27.

57. Pecaut MJ, Nelson GA, Gridley DS. Dose and dose rate effects of whole-body gamma-irradiation: I. Lymphocytes and lymphoid organs. In Vivo 2001; 15:195–208.